Energy 241 (2022) 122941

Contents lists available at ScienceDirect

Energy

journal homepage: www.elsevier.com/locate/energy

A comparative study on the turbulent explosion characteristics of syngas between CO-enriched and H_2-enriched

Z.Y. Sun [a, b, *], Shao-Yan LIU [a]

[a] Hydrogen Energy and Space Propulsion Laboratory (HESPL), School of Mechanical, Electronic and Control Engineering, Beijing Jiaotong University, Beijing, 100044, China

[b] Key Laboratory of Vehicle Advanced Manufacturing, Measuring and Control Technology (Beijing Jiaotong University), Ministry of Education, 100044, China

ARTICLE INFO

Article history:
Received 9 June 2021
Received in revised form
11 December 2021
Accepted 14 December 2021
Available online 16 December 2021

Keywords:
Syngas
Explosion characteristics
Turbulence
CO-Enriched
H_2-enriched

ABSTRACT

Syngas, containing mostly CO and H_2, has variant explosion properties for the specific contents. For a further understanding, a comparative study on the turbulent explosion characteristics of syngas between CO-enriched (the mole ratio of CO was 70%) and H_2-enriched (the mole ratio of H_2 was 70%) were conducted at different equivalence ratios (φ, from 0.4 to 3.0) and turbulent intensities (u'_{rms}, from 0 to 1.309 m/s). The peak value of maximum explosion pressure (p_{max}) was attained in the stoichiometric explosion of H_2-enriched syngas but in fuel-rich explosion of the CO-enriched, the growth extents of p_{max} seemed more sensitive to u'_{rms} for H_2-enriched syngas compared to CO-enriched syngas. The lowest values of explosion duration (t_c) was attained in fuel-rich explosions for both CO-enriched and H_2-enriched syngas but different corresponding φ to the lowest t_c, the phenomena were analyzed from the aspects of ignition delay time, laminar burning velocity, intrinsic instabilities, and flame/turbulence interaction. Finally, the pressure rising was comparatively observed, the maximum pressure rise rate ($(dp/dt)_{max}$) expressed more similar variation regulations to t_c rather than p_{max}, which meant flame propagation speed plays a more important role on the evolution of pressure rising.

1. Introduction

Suffering from the foreseeable depletion of fossil fuels, exploring and applying renewable fuel(s) becomes one uttermost hot even urgent topic in the field of energy science [1]. Produced from various biomass (like organic waste, food waste, fibril waste and algal biomass), syngas (containing mostly CO and H_2) is widely regarded as one promising renewable fuel [2,3]. Via different technologies and feedstocks, besides the uncertain impurities, syngas has specific contents of CO and H_2 which results in different combustion properties (like laminar burning velocity and intrinsic instabilities) between the CO-enriched (the mole ratio of CO is more than H_2) and the H_2-enriched (in which the mole ratio of H_2 is more than CO) [4–6]. Prior to a bulk application of syngas as a practical fuel, the fundamental combustion characteristics of CO/H_2 mixtures with the considerations of components effects should be highly concerned.

Forced ignition is one essential but crucial ignition manner in various power devices. Since it directly refers to the power capability of thermal devices (like internal combustion engines) and the hazardous potential of explosive materials, the behaviors after a forced ignition are significant for guiding a combustible mixture into practical applications [7]. Albeit bone-dry CO (i.e. CO without H_2, moisture, or in general H-containing species) would not be ignited at common conditions, the widest explosive limits and lowest ignition energy of H_2 could make CO/H_2 mixtures easily explosion [8] which would lead to public concern and fears on promoting syngas as a widely used fuel. Therefore, making fundamental studies on the explosion characteristics of CO/H_2 mixtures (especially considering the effects of dominant component) has practical significance.

Different to other fundamental combustion characteristics (like laminar burning velocity, intrinsic flame instability), the works about the explosion characteristics of 'syngas' are rare in the current literature. Within the past decade, State Key Laboratory of Explosion Science and Technology (China) [9] and Consiglio Nazionale delle Ricerche (Italy) [10,11] respectively studied the

* Corresponding author. Hydrogen Energy and Space Propulsion Laboratory (HESPL), School of Mechanical, Electronic and Control Engineering, Beijing Jiaotong University, Beijing, 100044, China.
E-mail addresses: sunzy@bjtu.edu.cn, zuoyu.sun@yahoo.com (Z.Y. Sun).

https://doi.org/10.1016/j.energy.2021.122941
0360-5442/

explosion properties of 'coal-derived syngas' (54.8% H_2, 6.6% CO, 24% CH_4 in mole fraction ratio) and 'wood-derived syngas' (2.0% ~3.0% H_2, 24%~60% CO, few CH_4), but the *arbitrary* components in *individual syngas* hardly reveal the explosion characteristics of CO/H_2 mixtures comprehensively. State Key Laboratory of Multiphase Flow in Power Engineering (China) [12,13] and Beijing Key Laboratory of Powertrain for New Energy Vehicle (China) [14] respectively measured the explosion indices of moisty laminar CO/H_2 mixtures and dry turbulent CO/H_2 mixtures, but the equal component ratio (the mole ratio of CO to H_2 was fixed to 50:50 in the mentioned works) cannot tell out the component effects on the explosion. From the aspects of kinetic effects, the ignition of syngas might be dominated by the chemical reaction of H_2, the explosion characteristics of CO/H_2 mixtures still had been observed related to the mole ratio of CO to H_2 (at least in laminar conditions [15]). Furthermore, the studies about turbulent explosion characteristics of CO/H_2 mixtures are scarcer albeit practical explosions always occur in turbulence. Recently, Sun [14] and Li et al. [16] respectively studied the turbulent explosion process of CO/H_2 mixtures in a spherical vessel and in an obstructed tube, the H_2-enriched condition (the mole ratio of CO to H_2 was 20:80) was taken for comparative investigation in Li's work [16] but the results contained the coupling effects of channel structure. Upon the available literature, it could be known that fundamental studies on turbulent explosion of CO/H_2 mixtures still should be conducted for the development of both explosion science and the syngas industrial, and the effects of dominant component should be considered into.

The present investigation made a comparative study on the turbulent explosion characteristics of CO/H_2 mixtures between CO-enriched and H_2—enriched, the mole fraction ratio of H_2 in the CO-enriched mixtures was set at 30% (a common ratio in most national projects of hydrogen pipeline transportation) while 70% in the H_2—enriched (as the symmetrical proportion for comparative study). Albeit as a continuation of earlier works [4,14,15], there existed adequate differentiation of the present work as: (*i*) the turbulent explosion characteristics of CO/H_2 mixtures were discussed between CO-enriched and H_2-enriched conditions; (*ii*) the effects of turbulence were discussed together with the effects of fuel compositions and fuel concentrations; and (*iii*) the effects of ignition delay, laminar burning velocity, and the flame-front/turbulence interaction were taken into the discussion on explosion process.

2. Methodology

2.1. Experimental apparatus

The present study was carried out on a turbulent explosion workbench (as shown in Fig. 1 (a)). According to the functionalities, the workbench could be divided into five subsystems (as demonstrated in Fig. 1 (b)) as: (*i*) a closed vessel; (*ii*) the discharge subsystem; (*iii*) the turbulence control subsystem; (*iv*) the ignition subsystem; and (*v*) the data acquisition subsystem.

The closed vessel was employed to provide space for explosion. For ensuring a centrosymmetric and sufficient propagation of combustion wave, the inner space was designed into spherical type with the diameter was 380 mm (the corresponding net volume was 28.73 L).

The discharging subsystem, linked to the vessel by gas pipes, was employed to prepare the desired mixture within the vessel. It mainly consisted of vacuum pump (Pronotek PNK DP 020C), high-pressurized gas H_2 bottle, high-pressurized CO bottle, high-pressurized air bottle, gas pipes, and pressure relief valves. The employed air was synthesized by O_2 and N_2 with a mole ratio of 21:79, the purities of the employed O_2, N_2, H_2 and CO were 99.99%.

The turbulence control subsystem was employed to generate turbulence within the vessel and control the turbulent intensity. It mainly consisted of four independent sets of motor-fan-porous plant (MFP), the four sets of MPF were mounted on the vessel into a configuration of pyramid whose geometric center was located at the vessel's center (for ensuring isotropic turbulence in the center). Each set of MFP contained one electronic motor, one metal fan, one porous plant, one magnetic coupling, and one frequency converter. The electronic motor was driven by the frequency converter, the magnetic couplings were employed to link the fans and the electronic motors via the wall of vessel for avoiding leakage during experiments. The rotation of fan generated a forward swirl whom would be transformed into multiple gas jets when it passed through the porous plant. If the four fans rotated with a same speed and a same rotation direction (as operated in the present work), the gas jets with same characters would be released from the four porous plants and then collided with each other at the vessel's center to form isotropic turbulence. The turbulent intensity (u'_{rms}, defined as the root-mean-square velocity of the flow at the vessel's center) was controlled by fan's speed, and it was measured by hot-wire anemometer prior to experiments. More detailed information about turbulence generation and control was available in literature [17—20].

The ignition subsystem was employed to a forced ignition of CO/H_2 mixtures at the vessel's center. It mainly consisted of a pair of electrodes (tungsten material, with a diameter of 2.5 mm), the ignition coil, and one power supply. The electrodes were oppositely located with a gap of 2 mm, and the location center was the geometrical center of the inner vessel to realize a central ignition.

The data acquisition subsystem was employed to measure and record the variation of pressure near the vessel's inner wall in the real-time. It mainly consisted of a piezoelectric pressure transducer (Kistler 89 6052-C, located at the bottom of the vessel), a charge amplifier (Kistler 5018-B, linked to pressure transducer by cable), a digital oscilloscope (Tektronix 3054), and a computer. Learnt from the previous works about laminar explosion characteristics reported by Huang's team [21—23], the sampling frequency in the present work was set at 100 kHz.

2.2. Experimental procedure

Each set of explosion experiment was carried out by a four-step procedure as:

Step 1: the preparation of desirable mixture in the vessel. Into an empty vessel, H_2, CO, and air were successively discharged to make up a mixture of H_2/CO/air with desirable equivalence ratio (φ, defined as the actual mass ratio of air-fuel to the mass ratio of air-fuel for a complete combustion) and mole ratio of CO to H_2 upon Daltons law of partial pressures. For covering the conditions of fuel-lean, stoichiometric, and fuel-rich, eleven different equivalence ratios (from 0.4 to 3.0) were taken. It should be noted that an absolute empty space cannot be realized in the experiments, 5.0 kPa was taken as the criterion of vacuum in all the experiments and such partial pressure was accounted into the amount of air.

Step 2: the construction of the initial turbulent condition. Once the mixtures had been prepared, the turbulence control subsystem would be started for stirring the mixtures and generating desirable turbulence. Like that reported by Zhao et al. [24,25] for the similar concept (the turbulence was measured by PIV), the turbulence generated by fan-stirred could be regarded as isotropic turbulence in the central zone of vessel, and the turbulence would be stable after a period of fan rotation. In the present work, the turbulent intensity (u'_{rms}) at the vessel's

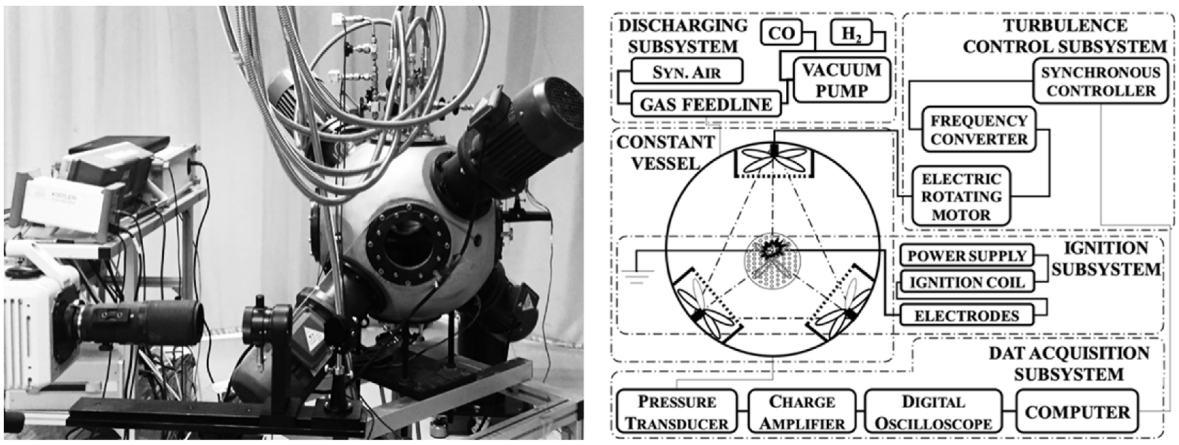

Fig. 1. The experimental workbench: (a) actual scene; and (b) schematic diagram.

center after a period of 3 min from the operation was linear to the fan speed as demonstrated in Fig. 2.

Step 3: the forced-ignition and the capture of explosion overpressure. After a period of three minutes from the operation, synchronous signals were released to triggerd both the ignition subsystem and the data acquisition subsystem. A forced-ignition of the mixture occurred at the vessel's center, and the variation of pressure near the inner wall would be collected real-time.

Step 4: the removal of exhaust and the preparation for the next experiment. After explosion, the gas pipes were opened to release high-pressure out the vessel; subsequently, high pressure air was charged and then again released from the pipe to removal the residual. After three (for CO-enriched explosion) and/or five (for H_2-enriched explosion) repetitions, the vessel was pumped into vacuum by the vacuum pump for the preparation of the next set of experiment.

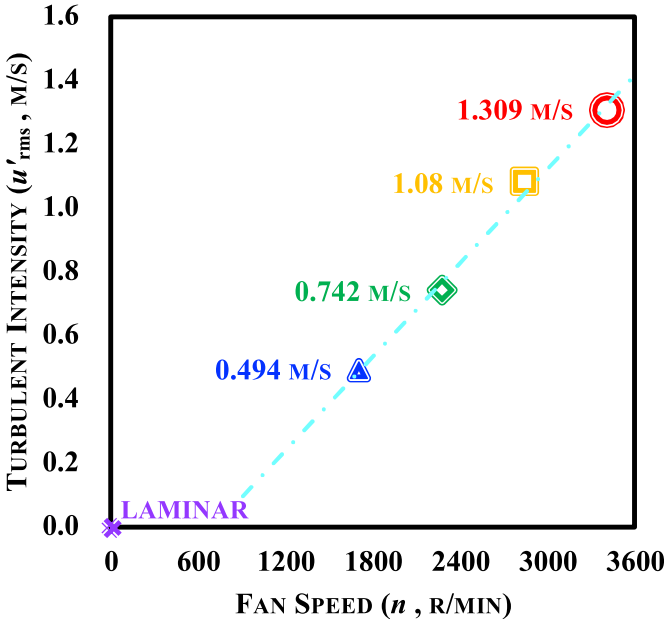

Fig. 2. The nexus between the turbulent intensity (at the vessel's center) and fan speed.

2.3. Parameters' definitions

Learnt from previous literature about laminar explosion characteristics [26–30], the explosion characteristics were always indicated by three essential indices:

The maximum explosion pressure (p_{max}) is the peak value of pressure reached in a closed vessel explosion, which could directly describe the features of an actual explosion in capability.

The explosion duration (t_c) is the time interval from ignition to the moment when p_{max} was attained, which could directly describe the evolution of an explosion and then reflect the reaction speed of the combustible mixtures in the air under the specific condition(s).

The maximum pressure rise rate ($(dp/dt)_{max}$) is the peak value of the pressure rise rate during an explosion process, which could indicate assessing the risk potential of a combustible mixture in enclosures.

For making the results available for comparative studies by other scholars, the present work also took the three indices to study the turbulent explosion characteristics. It should be noted that, in the present work, the values of p_{max} were obtained from the smoothed p-v. s.-t curves, and the smoothing criterion was second-order Savitsky-Golay equation learnt from the works about laminar explosion reported by Razus's team [26–29].

3. Results and discussion

3.1. Comparisons of explosion pressure

For a preliminary comparison on the explosion characteristics, the raw evolution curves (directly recorded by piezoelectric pressure transducer) of overpressure (p, the measured value of pressure near the vessel's inner wall) were taken to be compared. Fig. 3 and Fig. 4 respectively demonstrated the p-v. s.-t curves of CO-enriched and H_2-enriched mixtures with different equivalence ratios and different turbulent intensities under standard condition (p_{int} = 0.1 MPa and T_{int} = 300 K). Three remarkable phenomena could be observed as:

(i) In each studied explosion (no matter which component was the major, or what the value of φ was), the overpressure would rise after a period of 'constant initial value' and then decline from the maximal values. Such phenomenon had been excessively reported in nearly all the literature about the centrally-

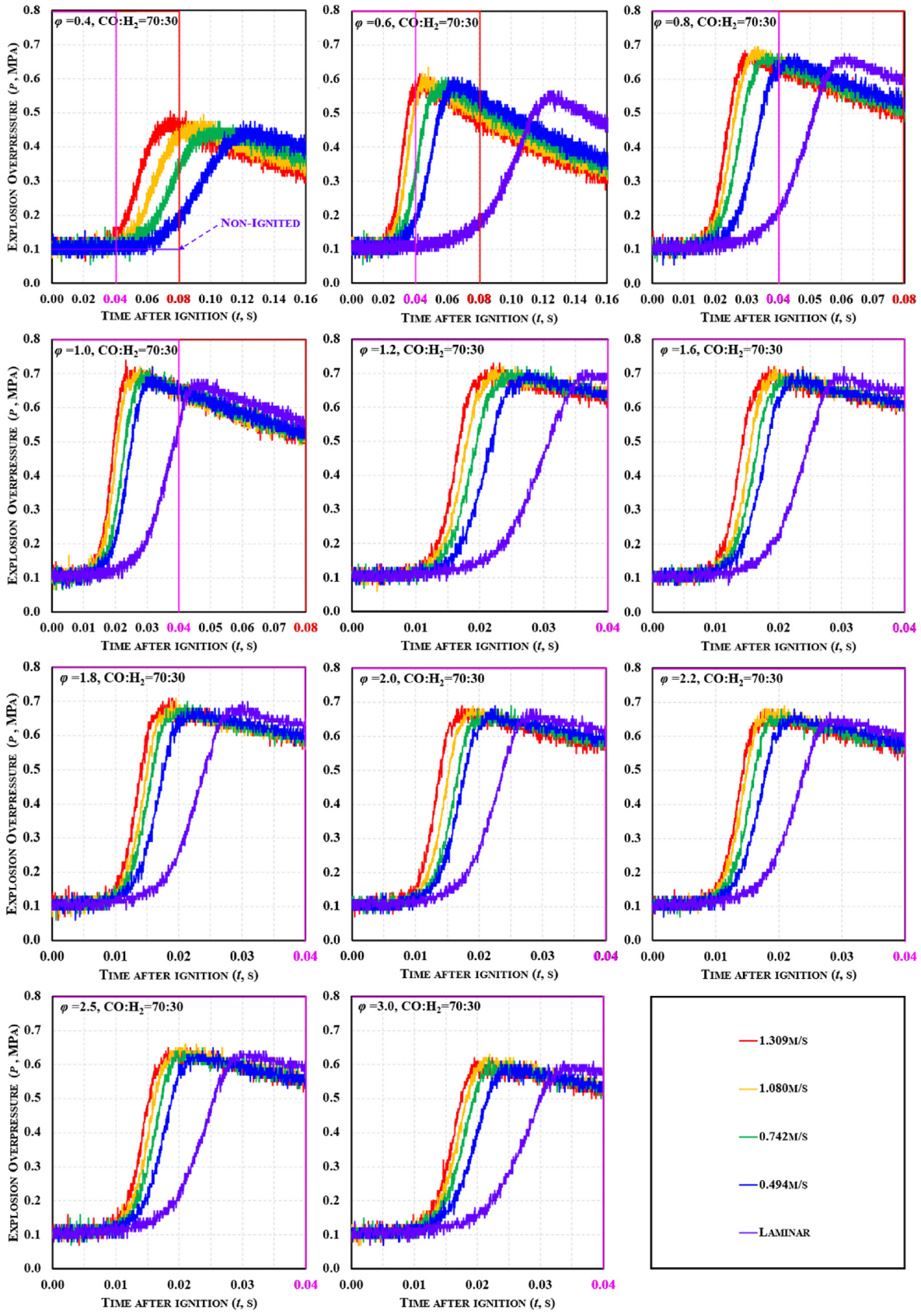

Fig. 3. Evolutions of overpressure during the turbulent explosion of CO-enriched mixtures.

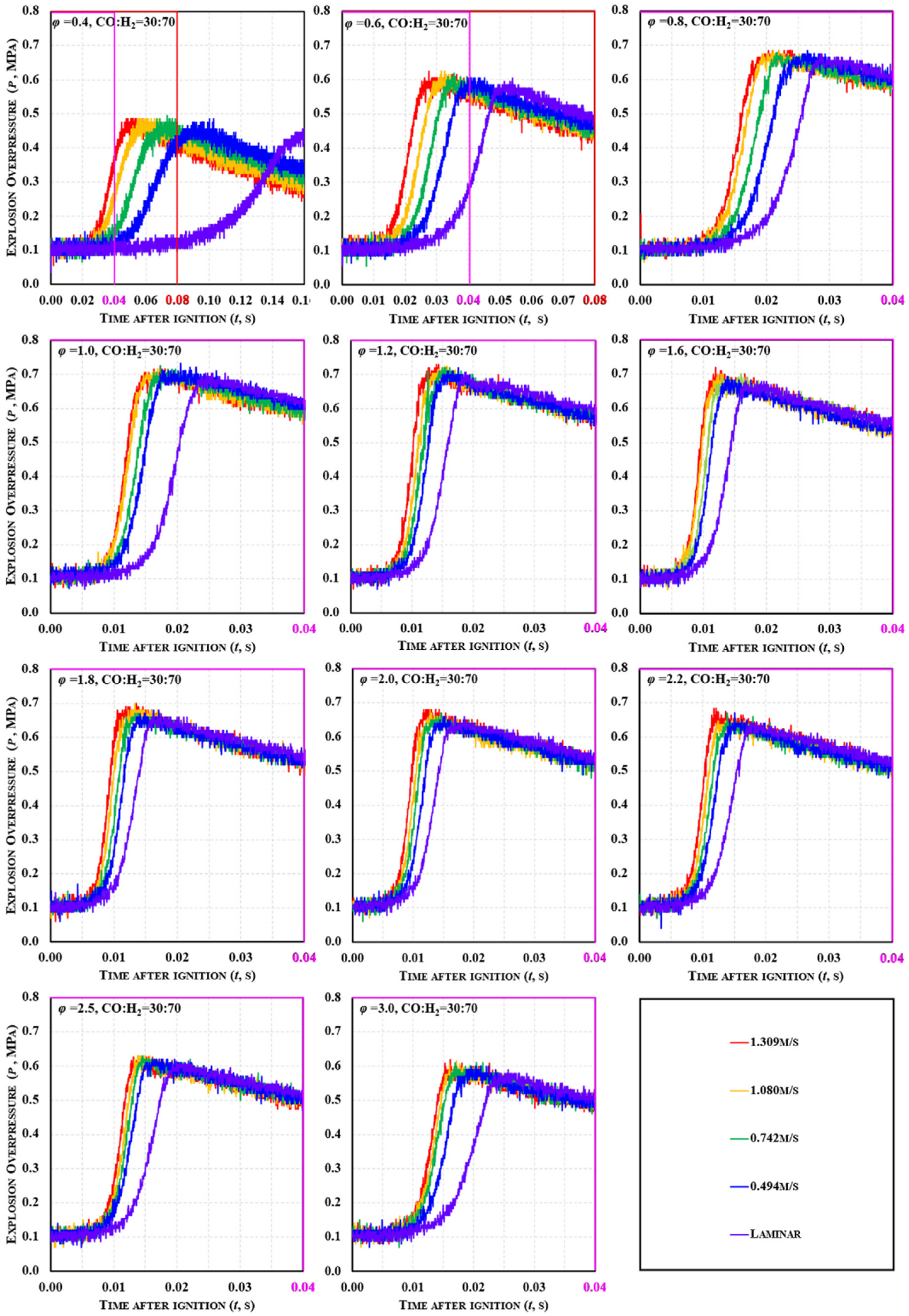

Fig. 4. Evolutions of overpressure during the turbulent explosion of H_2-enriched mixtures.

ignited explosion within vessels, the initial constant period was owing to the combustion wave was still far away the inner wall, the rapid rising was attributed to the continuous heat release, and the final decline was attributed to the maintaining heat loss after explosion via the vessel's wall.

(*ii*) To each studied turbulent ambience, the values of p_{max} and t_c were sensitive to fuel concentration. To fuel-lean (in which $\varphi < 1$) and stoichiometric explosions, with the increase of φ, the value of p_{max} rose and the corresponding t_c (to p_{max}) was advanced. However, to fuel-rich explosions (in which $\varphi > 1$), with the further remarkable increase of φ, p_{max} declined, but the corresponding t_c first was advanced and then delayed. Such phenomena occurred in both CO-enriched and H_2-enriched mixtures, just as the effects of equivalence ratio on laminar explosion characteristics [15].

(*iii*) To each specific equivalence ratio (no matter CO-enriched or H_2-enriched), with the increase of turbulent intensity (u'_{rms}), the value of p_{max} was raised and the corresponding t_c was advanced. To CO-enriched conditions, the mixture could hardly be ignited under laminar in the case of $\varphi = 0.4$ but it was easy to explode under turbulence and/or with higher concentration in laminar. The results indicated inducing turbulence seemly obtained similar effects to increasing H_2 in the mixture.

From the mentioned intuitive comparisons, the impacts of turbulence, fuel concentration and fuel components on the explosion of CO/H_2 mixtures seemed independent. For further and detailed insights, the variations of p_{max} to u'_{rms} and φ had been compared between CO-enriched and H_2—enriched explosions (as demonstrated in Fig. 5).

From the nexus among p_{max}, φ and u'_{rms} for the explosion of CO/H_2 mixtures, some interesting phenomena could be observed as:

(*i*) To H_2-enriched mixtures, the highest value of p_{max} was attained at stoichiometric explosion; however, to CO-enriched mixtures, the highest value of p_{max} was attained when the fuel concentration was a little rich ($\varphi = 1.2$).

(*ii*) To fuel-lean and stoichiometric mixtures, under a same initial condition, the values of p_{max} in H_2-enriched explosions were obviously higher than those in CO-enriched explosions; however, the results weren't effective to fuel-rich explosions.

(*iii*) To each studied mixture with specific fuel component and fuel concentration, with the increase of u'_{rms}, the value of p_{max} expressed linear growth; the growth rate was obviously related to both fuel component and fuel concentration.

The energy capability released by explosion is determined by chemical reaction, a specified condition (same fuel component, fuel concentration and initial thermodynamic ambience) corresponds a fixed adiabatic explosion pressure (p_{ad}, the theoretical value of pressure released by an equilibrium explosion), namely a fixed energy capability theoretically. Learnt from the previous measurements of p_{max} in laminar H_2 explosions (reported by Huang's team [30]) and laminar CO/H_2 mixtures (with CO:H_2 = 50:50, reported by Sun's team [14]), the peak value of p_{max} for H_2 was attained around the stoichiometric but attained around $\varphi = 1.2$ for the cases of CO/H_2 = 50:50. Without the consideration of turbulence effects, the results could be explained by the nexus between adiabatic flame temperature (T_{ad}, the temperature of the products when there are no heat losses to the surrounding environment and all of the energy released from combustion is used to heat the products) and fuel concentration. Since CO has a higher T_{ad} than H_2 and the peak value of T_{ad} for CO was attained around $\varphi = 1.2$, the higher carbon content made the fuel-rich explosion CO-enriched mixtures have higher values of T_{ad} than the stoichiometric explosion of H_2-enriched mixtures. Compared with the reported p_{max} of CO/H_2 mixtures with a mole ratio of 50:50 [14], it could be observed that the corresponding φ to the peak value of p_{max} is determined by the component of CO once the mole ratio of CO no less than H_2, and the presence of turbulence seemed hardly change such essence.

During an actual explosion, the exergy would be lost for heat conduction, mass diffusion, chemical reactions, and incomplete combustion (as reported by Han's team [31–33]); therefore, the obtained value of p_{max} is lower than p_{ad} due to the lost partial amount. With the presence of turbulence, the mass diffusion would be enhanced, the completion level of combustion would be raised, and the heat conduction would be reduced for the shortened duration to the accumulated heat flux via the wall. With the increase of u'_{rms}, the exergy loss during explosion would be reduced,

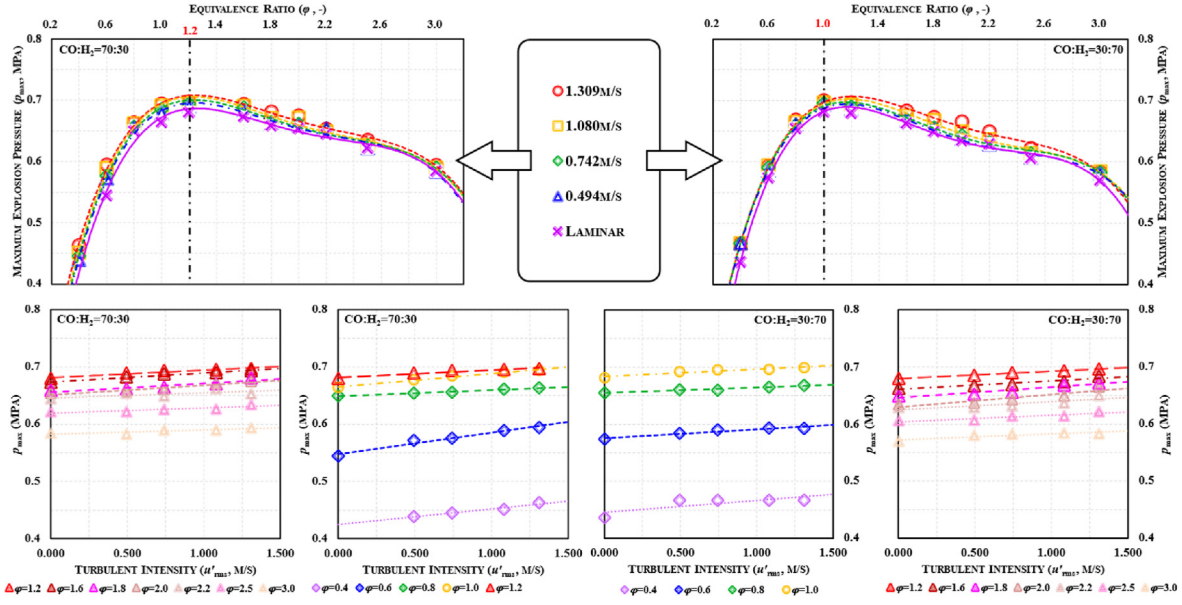

Fig. 5. Variations of p_{max} to different factors in the turbulent explosion of CO/H_2 mixtures.

the reduced drop of p_{max} from p_{ad} resulted in the growth of p_{max} (towards the value of p_{ad}).

3.2. Analyses of explosion duration

Fig. 6 demonstrated the explosion duration of syngas explosion with different initial conditions in the employed vessel. As could be observed, to fuel-lean explosions, with the increase of u'_{rms} and/or the increase of φ, the values of t_c (at any specific φ) would decline and the corresponding decline rates would be reduced, which was irrelevant to the major component in the mixture. However, to fuel-rich explosions, the variation regulation of t_c was nonmonotonic to φ (as reflections to the interactions of equivalence ratio and the major component) albeit it still was inversely proportional to u'_{rms}. The comprehensive effects of fuel components and turbulence made a critical equivalence ratio (φ_{cr}) to the minimum value of t_c under each studied turbulent ambience, such φ_{cr} in CO-enriched explosions was approximately 2.0 when the value of u'_{rms} is no more than 0.500 m/s but would be reduced to about 1.8 with the increase of u'_{rms}; in H_2-enriched explosions, the φ_{cr} was approximately 1.8 under laminar but it was observed about 1.6 under turbulence.

The continuation of an explosion is supported by chemical reaction, the explosion duration should be related to the activity of chemical kinetics. Under standard condition (employed in the present work), bone-dry CO would not be ignited, the chemical reaction of H_2 could be regarded as one important trigger to the ignition of CO/H_2 mixtures. To the component of H_2, the temperature of standard condition (300 K) even the temperature of initial conduction zone of H_2/air reaction would be lower than the crossover temperature (at which the chain-branching rate equals the chain-breaking rate, 1000 K under 0.1 MPa [34]), fuel-rich condition would be easier ignited for the faster consumption of H produced in the branching mechanism. Compared to CO-enriched mixtures with a same φ, H_2-enriched mixtures would provide more available H atoms to the reaction step of $H + O_2 \rightleftarrows O + OH$ which could enhance the reactivity of the explosion [35]; therefore, richer amount of hydrogen (-blended) mixtures would have a shorter ignition delay time [36], which resulted to a shorter explosion duration.

To a practical explosion process within confinement, the explosion duration is the direct result of the competition between space size (fixed in the present work) and flame propagation speed which is determined by the comprehensive effects of laminar burning velocity and the intrinsic instabilities [37]. Under standard condition, the fastest laminar burning velocity of H_2 was around 3.00 m/s (attained at $\varphi = 1.7–1.8$ [38,39]) which is about 15 times higher than CO (around 0.19 m/s attained at $\varphi = 1.6$ [39,40]); therefore, the H_2-enriched explosions had lower t_c and the φ_{cr} were much closer to the corresponding equivalence ratio of the fastest laminar burning velocity in pure H_2. Albeit the φ_{cr} to the fastest laminar burning velocity in CO was a little unricher than pure H_2, a little addition of H_2 into CO would induce the obvious variation of φ_{cr} (like moved to about 2.5 in CO:H_2 = 95:5, fallen into the range of 2.0–2.5 in CO:H_2 = 75:25, reported by Sun et al. [41]) due to the significant effects on the reaction of OH with CO during the combustion of CO/H_2 into air. Therefore, the φ_{cr} to the minimal value of t_c in CO-enriched explosions was richer than H2-enriched

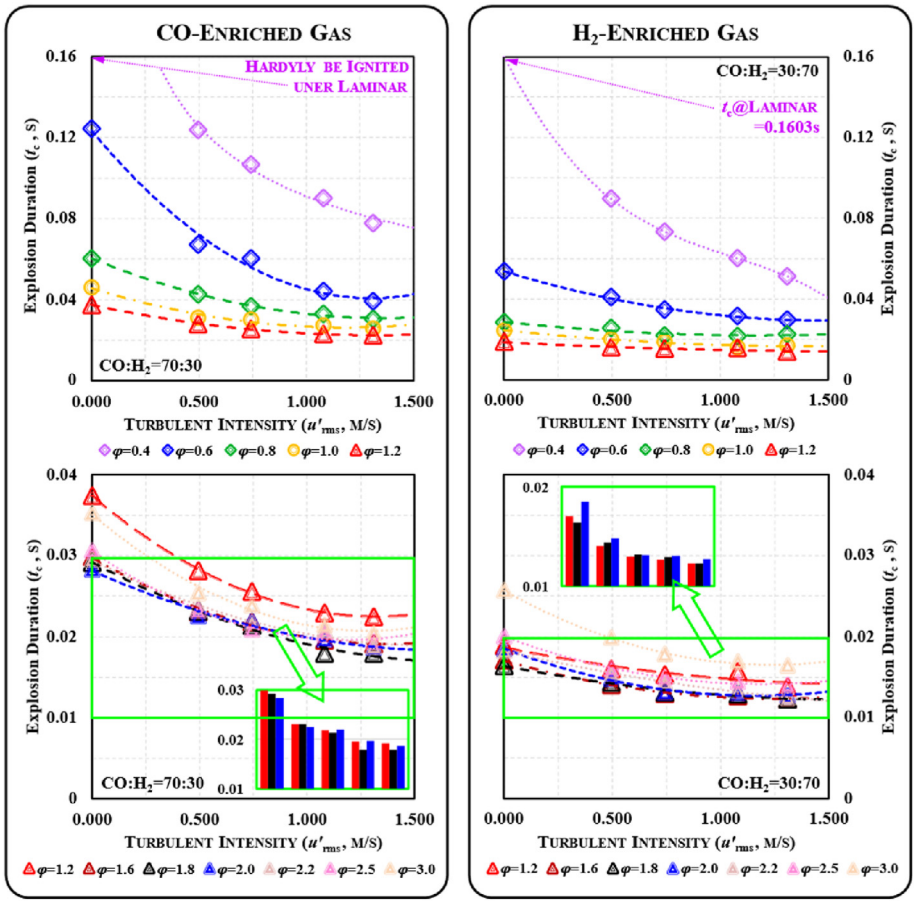

Fig. 6. Explosion durations of the turbulent explosion in CO/H_2 mixtures.

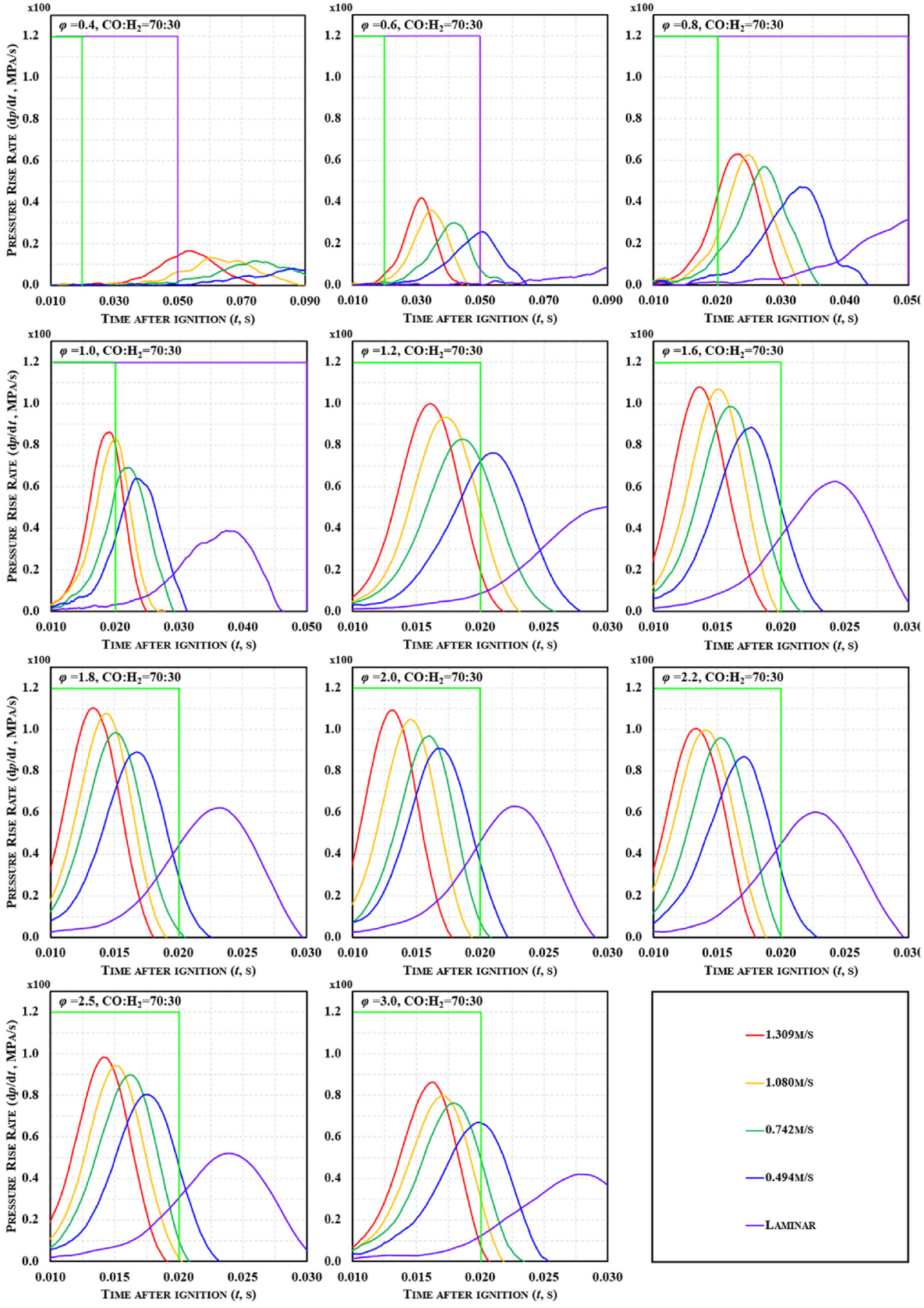

Fig. 7. Evolutions of pressure rise rate during the turbulent explosion in CO-enriched mixtures.

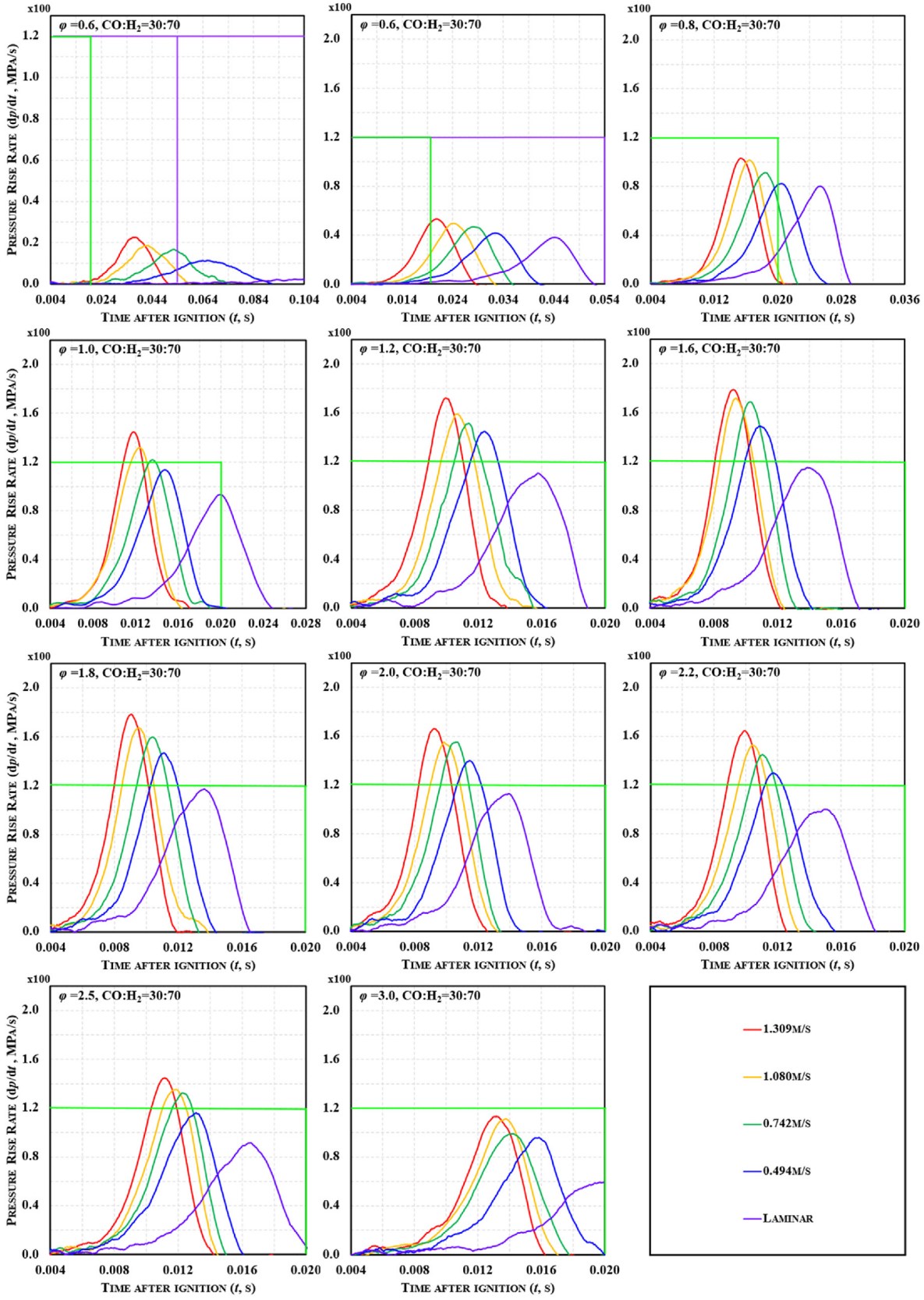

Fig. 8. Evolutions of pressure rise rate during the turbulent explosion in H_2-enriched mixtures.

explosions as be reflected to the φ_{cr} to the fastest laminar burning velocity.

From the aspect of intrinsic instabilities, under standard condition, stoichiometric and fuel-rich H_2/air premixed flames just suffer hydrodynamic instability, while fuel-lean H_2/air premixed flames suffer both hydrodynamic instability and diffusion-thermal instability. Hydrodynamic instability could not express remarkable effects to self-wrinkling until the flames had developed to sufficiently large (far larger than the size of the vessel employed by the present work) [42]. To fuel-rich and stoichiometric explosions, the presence of turbulence could corrugate the flame-front by the flame-front/eddies interaction and the enhanced hydrodynamic instability, the surface area would be enlarged and the flame speed would be correspondingly raised; to fuel-lean explosions, the presence of turbulence significantly promotes the mass diffusion of reactant to enhance the diffusion-thermal instability, the preferential effects of diffusion-thermal seriously wrinkled the flame-front to raise the flame speed.

Since the time scale in the flame thickness over flame speed would be remarkably higher than the turnover time of the eddies to the integral scale [43], the interaction between flame-front and turbulent eddies would be weak, which was experimentally observed from the related oscillation of flame structure in stoichiometric and fuel-rich turbulent H_2/air premixed flames [19]; therefore, to stoichiometric and fuel-rich explosions, the shortening of explosion duration might be mainly dominated by the enhanced hydrodynamic instability. To fuel-lean explosions, the flame thickness is related thicker while the flame speed is relatively lower, the time scale to flame-front would be longer than that in stoichiometric and fuel-rich explosions, the eddies effects on the corrugation of flame-front would be corresponding weaker; therefore, the shortening of explosion duration might be attributed to the enhanced diffusion-thermal instability since its preferential effects with the comparation of hydrodynamic instability under standard condition, which also expressed as the decline extent of t_c in fuel-lean explosions wider than that in stoichiometric and fuel-rich explosions.

Comparing the variations of t_c induced by turbulent intensity between CO-enriched and H_2-enriched explosions in fuel-rich mixtures, the component effects would be more obvious. Compared to the CO-enriched, H_2-enriched flame with a same fuel-rich equivalence ratio has a thinner flame thickness and a faster flame speed, the time response to the flame-front would be resultantly shorter in a same turbulent ambience, and the flame corrugation induced by the flame-front/turbulence interaction would be correspondingly stronger. Meanwhile, the presence of turbulence enhances the hydrodynamic instability and their coupling effects were considered as positive related to the hydrodynamic instability itself [19]. Therefore, to the fuel-rich H_2-enriched mixtures, the value of φ_{cr} would be reduced towards the range of 1.0–1.6 (the equivalence ratios correspond to the peak density ratio and the lowest laminar flame thickness in H_2) under stronger turbulent ambient.

To fuel-lean explosions, the stronger mass diffusion of H_2 than CO makes the non-equality between mass diffusion and heat diffusion higher in H_2-enriched explosions [44], coupling with the improvement of mass diffusion by turbulence, the local flame speed would be significantly accelerated. And thus, the variations of explosion duration in fuel-lean explosions to turbulent intensity were more sensitive to H_2-enriched mixtures as be reflected to the enhanced diffusion-thermal instability.

3.3. Variations on pressure rising

Fig. 7 and Fig. 8 respectively demonstrated the evolutions of pressure rise rate (dp/dt-v.s.-t curves) during the turbulent explosions in CO-enriched and H_2-enriched mixtures. As could be observed, the variations of dp/dt-v. s.-t curve to u'_{rms} and φ liked those of p-v. s.-t curves, namely, raising u'_{rms} could lead to the growth of maximum pressure rise rate ($(dp/dt)_{max}$) associated with advanced corresponding moment, and critical φ to the highest value of $(dp/dt)_{max}$ would exist. From the definition of dp/dt, it could be understood related to both explosion overpressure and explosion duration; therefore, the distinctive critical values of φ corresponding to p_{max} and t_c would make the ascertaining of dominant role (out from p_{max} and t_c) on $(dp/dt)_{max}$ interesting and valuable.

The nexus among $(dp/dt)_{max}$, u'_{rms} and φ for the explosions of studied syngas explosions were demonstrated in Fig. 9. As could be observed, with the increase of φ in the whole explosive range, the

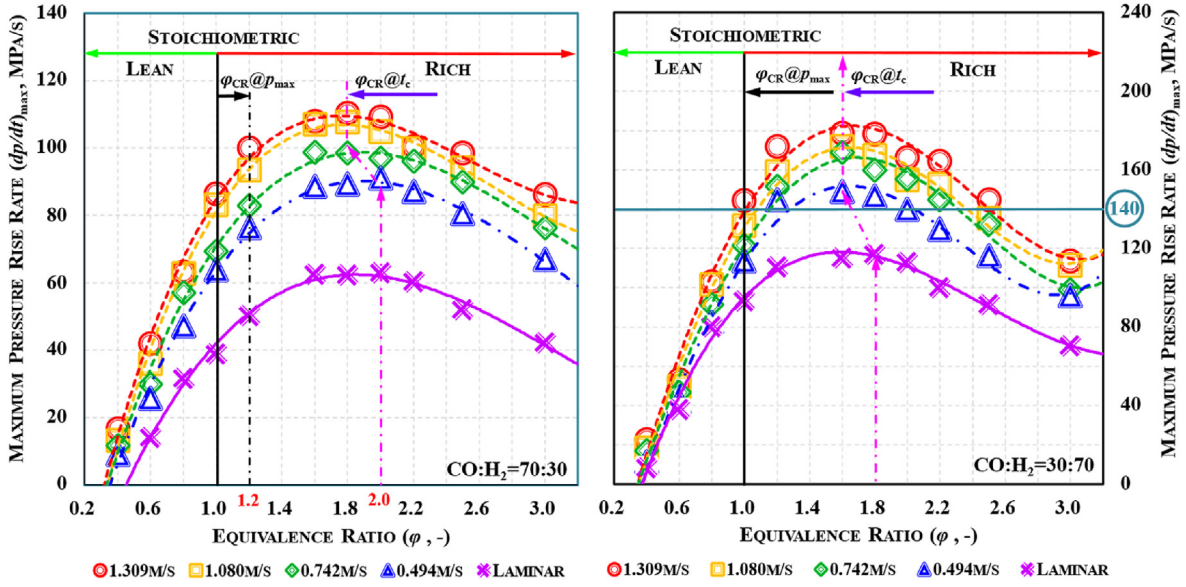

Fig. 9. Nexus among $(dp/dt)_{max}$, u'_{rms} and φ for the turbulent explosion of CO/H_2 mixtures.

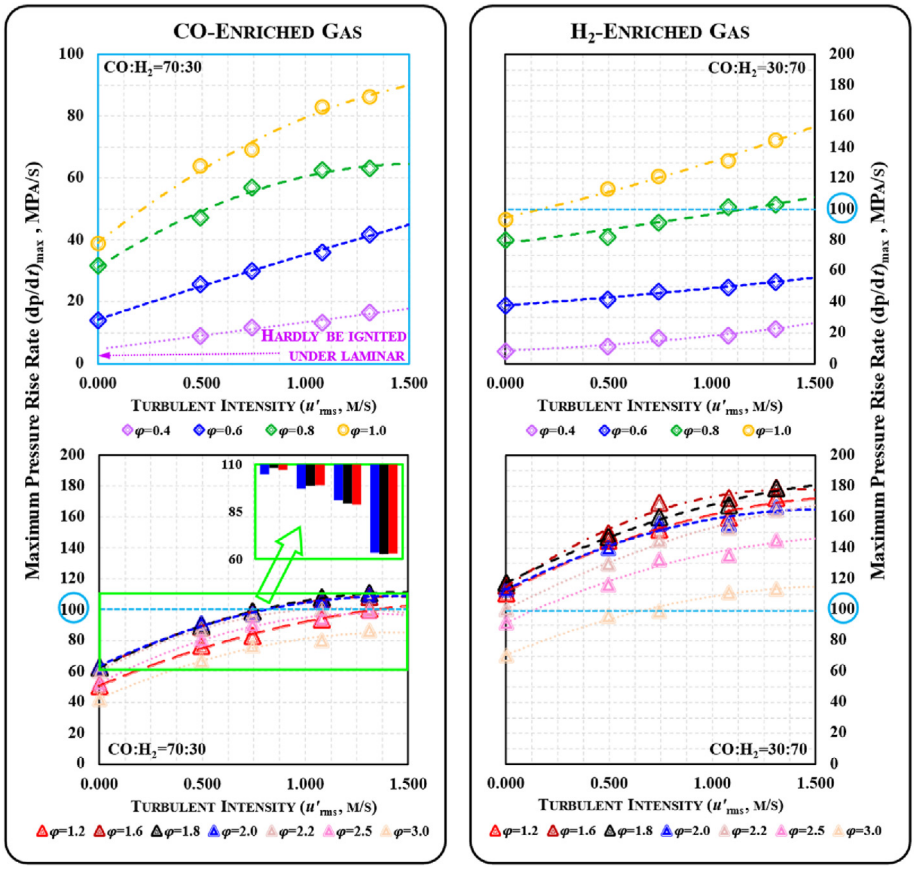

Fig. 10. Variations of maximum pressure rise rate for the turbulent explosion of CO/H_2 mixtures.

values of $(dp/dt)_{max}$ firstly rose and then declined.

Albeit the critical φ to the peak $(dp/dt)_{max}$ was different for different fuel components and/or turbulent intensities, a common law could be summarized that the critical φ to the peak $(dp/dt)_{max}$ was attained at the critical φ to the lowest t_c (no matter whether it was fixed to u'_{rms} or component). Such results indicated that the pressure rising process in turbulent explosion is dominated by flame speed.

For clearer insights on the impacts of turbulence on the maximum pressure rise rate, the $(dp/dt)_{max}$-v.s.-u'_{rms} curves were plotted in Fig. 10. As could be observed, the variations of $(dp/dt)_{max}$ to u'_{rms} could be considered as second-order polynomial, and the variation extent was determined by both u'_{rms} and φ. To fuel-rich explosions, the expressed parallel curves indicated that turbulence played a more important role on $(dp/dt)_{max}$ than fuel concentration, and such behaviors were insensitive to the major component in the CO/H_2 mixtures.

However, to fuel-lean and stoichiometric explosions, the variation regulations of $(dp/dt)_{max}$ to u'_{rms} expressed obvious differences between CO-enriched mixtures and H_2-enriched mixtures as: (*i*) in CO-enriched mixtures, the growth extent of $(dp/dt)_{max}$ induced by turbulence was gradually reduced with the increase of u'_{rms}; and (*ii*) in H_2-enriched mixtures, the growth extent of $(dp/dt)_{max}$ induced by turbulence was gradually raised with the increase of u'_{rms}. Such different behaviors were supposedly related to the interactions between turbulence and intrinsic instabilities whom in the fuel-lean explosions are stronger than in the fuel-rich explosions due to the preferential diffusion-thermal effects (as mentioned in the above).

It should be stated that turbulent flame speed, flame corrugation, the interactions of turbulence on instabilities, and the heat loss during explosion are crucial impacts on the mechanism of turbulent explosion, which could be studied in future works for a better understanding on explosion characteristic.

4. Conclusions

The present work made a comparative study on turbulent explosion characteristics of CO/H_2 mixtures between CO-enriched (the mole ratio of CO was 70%) and H_2-enriched (the mole ratio of H_2 was 70%) with different equivalence ratios (φ, from 0.4 to 3.0) and turbulent intensities (u'_{rms}, from 0 to 1.309 m/s) under standard condition. Main conclusions were summarized as the follows:

(a) The peak value of maximum explosion pressure (p_{max}) was attained in the stoichiometric H_2-enriched mixtures but in fuel-rich (the corresponding φ was about 1.2) CO-enriched mixtures. With the increase of u'_{rms}, p_{max} monotonously rosed in the linear, the growth extent in fuel-rich explosions seemed highly sensitive to u'_{rms} for the H_2-enriched mixtures.

(b) The lowest value of explosion duration (t_c) was attained in fuel-rich mixtures for both CO-enriched and H_2-enriched syngas, but the corresponding φ were different. With the increase of u'_{rms}, the value of t_c would be reduced, and the decline rate extent became narrow with the increase of φ. The effects of H_2 amount on the ignition delay time and the enhancement of flame instabilities induced by turbulence were regarded play more important roles than the flame corrugation caused by eddies.

(c) The maximum pressure rise rate ($(dp/dt)_{max}$) expressed more similar variation regulations to t_c rather than p_{max}, namely, flame speed played the dominant role on the evolution of pressure rising. Since the interaction of turbulence and intrinsic instabilities were more significant to H_2 premixed flames, the variations of $(dp/dt)_{max}$ to u'_{rms} were more noticeable in H_2-enriched explosions.

Credit author statement

Z. Y. Sun: Conceptualization, Methodology, Investigation, Data curation, Writing – original draft preparation, Reviewing and Editing. Shao-Yan Liu: Investigation, Data curation, Reviewing and Editing

Declaration of competing interest

The authors declare that they have no known competing financial interests or personal relationships that could have appeared to influence the work reported in this paper.

Acknowledgements

This research was financially supported by National Natural Science Foundation of China [grant number 52076010]. Sincere thanks to all the editors and all the reviewers for their works on this article.

References

[1] Sun ZY, Li GX. On reliability and flexibility of sustainable energy application route for vehicles in China. Renew Sustain Energy Rev 2015;51:830–46. https://doi.org/10.1016/j.rser.2015.06.042.
[2] Richardson Y, Blin J, Julbe A. A short overview on purification and conditioning of syngas produced by biomass gasification: catalytic strategies, process intensification and new concepts. Prog Energy Combust Sci 2012;38:765–81. https://doi.org/10.1016/j.pecs.2011.12.001.
[3] Scarlat N, Dallemand JF, Fahl F. Biogas: developments and perspectives in Europe. Renew Energy 2018;129:457–72. https://doi.org/10.1016/j.renene.2018.03.006.
[4] Sun ZY. Turbulent explosion characteristics of stoichiometric syngas. Int J Energy Res 2018;42:1225–36. https://doi.org/10.1002/er.3922.
[5] Li HM, Li GX, Jiang YH. Laminar burning velocities and flame instabilities of diluted H_2/CO/air mixtures under different hydrogen fractions. Int J Hydrogen Energy 2018;43:16344–54. https://doi.org/10.1016/j.ijhydene.2018.06.132.
[6] Li HM, Li GX, Jiang YH, Li L, Li FS. Flame stability and propagation characteristics for combustion in air for an equimolar mixture of hydrogen and carbon monoxide in turbulent conditions. At Energ 2018;157:76–86. https://doi.org/10.1016/j.energy.2018.05.101.
[7] Li HM, Li GX, Li L, Yao ZP. Experimental study on thermal ignition and combustion of droplet of ammonium dinitramide based liquid propellant in different oxidizing gas atmospheres. Acta Astronaut 2020;169:40–9. https://doi.org/10.1016/j.actaastro.2019.12.030.
[8] Wang WQ, Sun ZY. Experimental studies on the explosive limits and minimum ignition energy of syngas: a comparative review. Int J Hydrogen Energy 2019;44:5640–9. https://doi.org/10.1016/j.ijhydene.2018.08.016.
[9] Ning JN, Wang C, Lu J. Explosion characteristics of coal gas under various initial temperature and pressure. Shock Waves 2006;15:461–72. https://doi.org/10.1007/s00193-006-0046-x.
[10] di Sarli V, Cammarota F, Salzano E. Explosion parameters of wood chip-derived syngas in air. J Loss Prev Process Ind 2014;32:399–403. https://doi.org/10.1016/j.jlp.2014.10.016.
[11] Basco A, Cammarota F, di Sarli V, Salzano E, di Benedetto A. Theoretical analysis of anomalous explosion behavior for H_2/CO/O_2/N_2 and CH_4/O_2/N_2/CO_2 mixtures in the light of combustion-induced rapid phase transition. Int J Hydrogen Energy 2015;40:8239–47.
[12] Xie Y, Wang J, Cai X, Huang Z. Pressure history in the explosion of moist syngas/air mixtures. Fuel 2016;185:18–25. https://doi.org/10.1016/j.fuel.2016.07.072.
[13] Xie Y, Wang X, Wang J, Huang Z. Explosion behavior predictions of syngas/air mixtures with dilutions at elevated pressures: explosion and intrinsic flame instability parameters. Fuel 2019;255:115724. https://doi.org/10.1016/j.fuel.2019.115724.
[14] Sun ZY. Explosion pressure measurement of 50%H_2-50%CO synthesis gas-air mixtures in various turbulent ambience. Combust Sci Technol 2018;190:1007–22. https://doi.org/10.1080/00102202.2018.1424141.
[15] Sun ZY. Laminar explosion properties of syngas. Combust Sci Technol 2020;192:166–81. https://doi.org/10.1080/00102202.2018.1558404.
[16] Li T, Hampp F, Lindstedt RP. The impact of hydrogen enrichment on the flow field evolution in turbulent explosions. Combust Flame 2019;203:105–19. https://doi.org/10.1016/j.combustflame.2019.01.037.
[17] Sun ZY, Li GX. Propagation speed of wrinkled premixed flames within stoichiometric hydrogen-air mixtures under standard temperature and pressure. Kor J Chem Eng 2017;34:1846–57. https://doi.org/10.1007/s11814-017-0084-3.
[18] Sun ZY, Li GX. Turbulent influence on explosion characteristics of stoichiometric and rich hydrogen/air mixtures in a spherical closed vessel. Energy Convers Manag 2017;149:1526–36. https://doi.org/10.1016/j.enconman.2017.07.051.
[19] Sun ZY. Structure of turbulent rich hydrogen-air premixed flames. Int J Energy Res 2018;42:2845–58. https://doi.org/10.1002/er.4048.
[20] Sun ZY. Experimental studies on the explosion indices in turbulent stoichiometric H_2/CH_4/air mixtures. Int J Hydrogen Energy 2019;44:469–76. https://doi.org/10.1016/j.ijhydene.2018.02.094.
[21] Tang C, Zhang S, Si Z, Huang Z, Zhang Z, Jin Z. High methane natural gas/air explosion characteristics in confined vessel. J Hazard Mater 2014;278:520–8. https://doi.org/10.1016/j.jhazmat.2014.06.047.
[22] Li Q, Cheng Y, Huang Z. Comparative assessment of the explosion characteristics of alcohol-air mixtures. J Loss Prev Process Ind 2015;37:91–100. https://doi.org/10.1016/j.jlp.2015.07.003.
[23] Hu E, Tian H, Zhang X, Li X, Huang Z. Explosion characteristics of n-butanol/iso-octane-air mixtures. Fuel 2017;188:90–7. https://doi.org/10.1016/j.fuel.2016.10.002.
[24] Zhao H, Wang J, Cai X, Dai H, Bian Z, Huang Z. Flame structure, turbulent burning velocity and its unified scaling for lean syngas/air turbulent expanding flames. Int J Hydrogen Energy 2021;46:25699–711. https://doi.org/10.1016/j.ijhydene.2021.05.090.
[25] Zhao H, Wang J, Cai X, Dai H, Huang Z. Turbulent burning velocity and its unified scaling of butanol/isomers/air mixtures. Fuel 2021;306:121738. https://doi.org/10.1016/j.fuel.2021.121738.
[26] Mitu M, Giurcan V, Razus D, Prodan M, Oancea D. Propagation indices of methane-air explosions in closed vessels. J Loss Prev Process Ind 2017;47:110–9. https://doi.org/10.1016/j.jlp.2017.03.001.
[27] Razus D, Mitu M, Giurcan V, Oancea D. Propagation indices of methane-nitrous oxide flames in the presence of inert additives. J Loss Prev Process Ind 2017;49:418–26. https://doi.org/10.1016/j.jlp.2017.08.010.
[28] Giurcan V, Mitu M, Razus D, Oancea D. Pressure and temperature influence on propagation indices of n-butane-air gaseous mixtures. Process Saf Environ 2017;111:94–101. https://doi.org/10.1016/j.psep.2017.06.020.
[29] Movileanu C, Gosa V, Razus D. Explosion of gaseous ethylene-air mixtures in closed cylindrical vessels with central ignition. J Hazard Mater 2012;235–236:108–15. https://doi.org/10.1016/j.jhazmat.2012.07.028.
[30] Tang C, Huang Z, Jin C, He J, Wang J, Wang X, Miao H. Explosion characteristics of hydrogen-nitrogen-air mixtures at elevated pressures and temperatures. Int J Hydrogen Energy 2009;34:554–61. https://doi.org/10.1016/j.ijhydene.2008.10.028.
[31] Zhang J, Huang Z, Han D. Exergy losses in auto-ignition processes of DME and alcohol blends. Fuel 2019;229:116–25. https://doi.org/10.1016/j.fuel.2018.04.162.
[32] Zhang J, Han D, Huang Z. Thermodynamic analysis for premixed hydrogen flames with diluents of argon/nitrogen/carbon dioxide. Int J Hydrogen Energy 2019;44:5020–9. https://doi.org/10.1016/j.ijhydene.2019.01.041.
[33] Zhang J, Huang Z, Han D. Effects of mechanism reduction on the exergy losses analysis in n-heptane auto-ignition processes. Int J Eng Res 2020;21:1764–77. https://doi.org/10.1177/1468087419836870.
[34] del Álamo G, Williams FA, Sánchez AL. Hydrogen-oxygen induction times above crossover temperatures. Combust Sci Technol 2004;176:1599–626. https://doi.org/10.1080/00102200490487175.
[35] Krejci MC, Mathieu O, Vissotski AJ, Ravi S, Sikes TG, Petersen EL, Kérmonès A, Metcalfe W, Curran HJ. Laminar flame speed and ignition dealy time data for the kinetic modeling of hydrogen and syngas fuel blends. J Eng Gas Turbines Power 2013;135:21503. https://doi.org/10.1115/gt2012-69290.
[36] Schultze M, Mantzaras J, Bombach R, Boulouchos K. An experimental and numerical investigation of the hetero-/homogeneous combustion of fuel-rich hydrogen/air mixtures over platinum. Proc Combust Inst 2013;34:2269–77. https://doi.org/10.1016/j.proci.2012.05.029.
[37] Sun ZY, Li GX. Propagation characteristics of laminar spherical flames within homogeneous hydrogen-air mixtures. At Energ 2016;116:116–27. https://doi.org/10.1016/j.energy.2016.09.103.
[38] Dahoe AE. Laminar burning velocities of hydrogen–air mixtures from closed vessel gas explosions. J Loss Prev Process Ind 2005;18:152–66. https://doi.org/10.1016/j.jlp.2005.03.007.
[39] Dong C, Zhou Q, Zhao Q, Zhang Y, Xu T, Hui S. Experimental study on the laminar flame speed of hydrogen/carbon monoxide/air mixtures. Fuel 2019;88:1858–63. https://doi.org/10.1016/j.fuel.2009.04.024.
[40] Wu F, Kelley AP, Tang C, Zhu D, Law CK. Measurement and correlation of laminar flame speeds of CO and C_2 hydrocarbons with hydrogen addition at atmospheric and elevated pressures. Int J Hydrogen Energy 2011;36:13171–80. https://doi.org/10.1016/j.ijhydene.2011.07.021.

[41] Sun H, Yang SI, Jomaas G, Law CK. High-pressure laminar flame speeds and kinetic modeling of carbon monoxide/hydrogen combustion. Proc Combust Inst 2007;31:439–46. https://doi.org/10.1016/j.proci.2006.07.193.
[42] Sun ZY, Liu FS, Bao XC, Liu XH. Research on cellular instabilities in outwardly propagating spherical hydrogen-air flames. Int J Hydrogen Energy 2012;37:7889–99. https://doi.org/10.1016/j.ijhydene.2012.02.011.
[43] Daniele S, Mantzaras J, Jansohn P, Denisov A, Boulouchos K. Flame front/turbulence interaction for syngas fuels in the thin reaction zones regime: turbulent and stretch laminar flame speeds at elevated pressures and temperatures. J Fluid Mech 2013;724:36–68. https://doi.org/10.1017/jfm.2013.141.
[44] Zhao H, Wang J, Bian Z, Cai X, Li X, Huang Z. Onset of cellular instability and self-acceleration propagation of syngas spherically expanding flames at elevated pressures. Int J Hydrogen Energy 2019;44:27995–8006. https://doi.org/10.1016/j.ijhydene.2019.09.038.